Journal of Fluorescence (2019) 29:1381–1392
https://doi.org/10.1007/s10895-019-02448-3

ORIGINAL ARTICLE

Bioimaging Applications of Carbon dots (C. dots) and its Cystamine Functionalization for the Sensitive Detection of Cr(VI) in Aqueous Samples

Roshni V.[1] · Varsha Gujar[1] · Heena Pathan[1] · Sehbanul Islam[2] · Madhumita Tawre[3] · Karishma Pardesi[3] · Manas Kumar Santra[2] · Divya Ottoor[1]

Received: 2 June 2019 / Accepted: 1 October 2019 / Published online: 20 November 2019

Abstract

In this study, one step hydrothermal synthetic strategy was adopted for preparing carbon dots (C. dots) from jeera (Cumin: *Cuminum cyminum*), a naturally abundant and cost effective carbon source. The physical, optical and surface functional properties of C. dots were extensively studied by different techniques such as Transmission electron microscopy (TEM), Scanning electron microscopy (SEM), spectrophotometry, fluorescence spectroscopy, Fourier transform infrared spectroscopy (FTIR) and X-ray diffraction (XRD). The obtained C. dots were highly water dispersible and photostable with a quantum yield of 5.33%. The antioxidant property of C. dots was investigated by 2, 2-diphenyl-1-picrylhydrazyl (DPPH) assay. The C. dots were then capped with cystamine using 1-(3-dimethylaminopropyl)-3-ethyl carbodiimide (EDC) and N-Hydroxysuccinimide (NHS) coupling chemistry to design a selective sensing system for chromium (VI) (Cr (VI)). The minimum detection limit of Cr (VI) was found to be 1.57 μM. Biocompatibility and low toxicity of C. dots obtained from jeera made it a potential tool for bioimaging application. The internalisation of C. dots by MCF-7 breast cancer cells and Multi Drug Resistant (MDR) pathogens such as *Staphylococcus aureus* and *Pseudomonas aeruginosa* were proved by the bioimaging of respective cells.

Keywords Carbon dots (C. dots) · Cumin seeds (jeera) · Fluorescence · Cr (VI) sensing · MCF-7 cells · Bioimaging

Introduction

The invention of highly fluorescent carbon nanoparticles synthesised from natural sources has helped the scientific community to overcome the limitations of organic dye and other synthetic fluorophores in various applications such as optical sensing, bio imaging etc. Among these nanoparticles, carbon dots (C. dots) has received a special attention owing to their remarkable features, of which, fluorescence characteristics, solubility, chemical and physical stability and biocompatibility are highly relevant for diverse applications [1–5]. Various natural and renewable sources have been employed for the green synthesis of C. dots as evident from recent literature reports [6, 7]. C. dots prepared from milk, potato, orange juice, jackfruit, coriander leaves, coconut milk, ground nut etc. are the few among them [8–14].

C. dots are nanometer sized particles mainly composed of sp^2 hybridised carbon core with various organic functional groups such as –COOH, -NH_2, -OH etc. on its surface. In order to apply C. dots as chemosensors for highly selective and sensitive detection, it is desirable to attach them with specific organic, polymeric or biological groups via covalent bonds, hydrogen bonds or electrostatic interactions. Application of capped quantum dots for the specific sensing of toxic metals even though reported, is a less explored area of optical sensing [15].

The capturing of images of biological matter by treating it with a fluorescent molecule to get easily explicable images is widely referred to as bioimaging. Presence of abundant

Electronic supplementary material The online version of this article (https://doi.org/10.1007/s10895-019-02448-3) contains supplementary material, which is available to authorized users.

✉ Divya Ottoor
divya@chem.unipune.ac.in

[1] Department of Chemistry, Savitribai Phule Pune University, Pune, India

[2] National Centre For Cell Science(NCCS), Pune, India

[3] Department of Microbiology, Savitribai Phule Pune University, Pune, India

hydrophilic surface functional groups, favourable optical properties, good biocompatibility, less toxicity etc. makes the C. dots eligible for bioimaging applications [16]. The wide emission ranges of C. dots enable it to be used as multicolour fluorescence imaging agent [17]. C. dots obtained from the spices has been applied for imaging of cancerous kidney cells as well as for the inhibition of tumour growth [18]. C. dots obtained from food waste were used for the imaging of liver carcinoma cells [19]. The rise in multi-drug resistant bacteria necessitated the researchers to develop detection system for bacterial species with high sensitivity and selectivity. The imaging of bacterial cells has its importance as it gives vital information about the shapes and functions of bacteria. *Staphylococcus aureus* and *Pseudomonas aeruginosa* are gram positive and gram negative bacteria respectively, that causes serious infections in human beings. The imaging of bacterial and fungal cells using C-dots from *Punica granatum* juice has been reported recently. The C. dots synthesised from apple juice were used for the imaging of bacterial and fungal cells [20, 21].

Sensitive detection of environmentally relevant toxic metal ions such as Cr (VI), its speciation and total Cr content in environmental samples is highly significant. Of the various reported sensing approaches [6], optical sensing methods using excellent fluorophores synthesised by green approach with environment friendly precursors are well suited for such studies. Herein, highly water dispersible C. dots were synthesised from jeera (Cumin: *Cuminum cyminum*) using one pot hydrothermal methodology. The added benefits of C. dots to be employed for such applications are their excellent water dispersibility, brilliant fluorescence properties, non-toxicity and photo stability. The photo physical and biological properties of the obtained C. dots were examined. The obtained C. dots are free from any hazardous chemicals as they prove negligible cytotoxicity. The antioxidant efficiency of C. dots were evaluated using DPPH assay and compared with the extract of raw jeera samples [22]. The fabrication of cystamine-C. dots (Cysm-C.dot) system using EDC/NHS coupling chemistry was carried out and its application towards the selective sensing of Cr(VI) was investigated. These biocompatible nanostructures are appropriate for medical applications also. The fluorescence and biocompatible properties make them the desirable candidate for imaging and drug delivery applications also. Hence, to showcase the multifunctional aspects of C. dots, bioimaging properties of probes were examined in which both human cancerous cells and bacterial cells were taken as model systems.

Experimental Details

Materials and Reagents

Cumin seeds, an easily available and widely used spice of Indian kitchen, were purchased from the local grocery shop and used without any treatment. No additives were used for the synthesis of C. dots. Cystamine was purchased from Sigma-Aldrich. EDC and NHS were obtained from SRL Pvt. Ltd., India. DPPH was obtained from Sigma-Aldrich. Cobalt Nitrate $Co(NO_3)_2$, Cadmium Nitrate $Cd(NO_3)_2$, Potassium dichromate $K_2Cr_2O_7$, Copper Sulphate $CuSO_4$, Nickel Nitrate($Ni(NO_3)_2$, Lead Nitrate $Pb(NO_3)_2$, Ferrous Sulphate ($FeSO_4$), Ferric Sulphate ($Fe_2(SO_4)_3$) and Mercuric Chloride ($HgCl_2$) were purchased from SDFCL. $NaH_2PO_4.2H_2O$ and $Na_2HPO_4.7H_2O$ were also purchased from SDFCL. These were used for preparing buffer solutions of different pH. Phosphate buffer (0.1 M) with pH 7.4 was used in the carbodiimide reaction. All the solutions were prepared in triple distilled water.

Instruments for Characterization of C. dots

Transmission electron microscopy (TEM- Tecnai G^2–20 Twin (FEI, Netherlands)) with an accelerating voltage of 200 KV was used for acquiring images of C. dots. Copper grid with carbon was used for drop casting in which the diluted solution of C.dot(0.01 mg/ml) was drop casted after ultra sonication (Ultra-sonicator -BRANSON-1800) and images were captured. Scanning electron microscopy (SEM - Model- Nova Nanosem 450) was used for finding the surface morphology of the obtained C. dots. The samples were drop casted on silicon wafare and spurt coated with platinum for better imaging (Sputter coater-Quorum-Q150T ES). The size distribution of C. dots was done by counting 50 particles. The absorption spectra were recorded in a Shimadzu UV–visible spectrophotometer with absorbance taken in a region of 200–600 nm using water as reference. Fluorescence measurements were recorded using Jasco FP-8300 spectro fluorimeter (with 150 W Xe lamp) in a 1 cm. optical pathway quartz cuvette. The excitation and emission slit width were 2.5 nm with a scan speed of 1000 nm/min and getting the data at 1 nm data interval. FTIR-8400, Shimadzu was used to record spectral data of the functional groups on the C.dot surface. The fluorescence life time measurements were carried out using Time correlated single photon counting (TCSPC) instrument (Horiba Jobin Yvon Inc., France). XRD of C. dots were obtained using a Rigaku Ultima IV powder X-ray diffractometer scanned in the range of 5^0–80^0 at a scan rate of 5^0/min. Zeta potential of C. dots were measured using Beckman coulter Delsa nano(scattering angle - 90^0, cell used- Acrylic Cell, PBS buffer concentration 0.1 M, pH 7.4). DLS was taken using Beckman coulter Delsa nano.

Synthesis of C. dots

1 g of jeera was washed, dried, powdered and dissolved in 30 ml of water. This solution was transferred into a 50 ml autoclave and kept for hydrothermal treatment for about 6 h

at a temperature of 250 °C. During hydrothermal heating, the jeera sample underwent various processes such as carbonisation, nucleation and polymerisation to obtain highly fluorescent C. dots. The process resulted in brown coloured solution with large sized carbonaceous matter which was removed by ultracentrifugation (8000 rpm, 15 min.) followed by filtration. The supernatant solution was lyophilised and dissolved in water to form a concentration of 1 mg/ml for further use.

DPPH Assay

Based on the literature, the methanolic extract of raw jeera showed good antioxidant property, so we evaluated the efficiency of C. dots obtained from jeera and compared with the former [22–26]. The antioxidant potential of C. dots were measured by DPPH free radical assay [22]. 10 mg/ml of stock solution of C. dots was prepared for performing the experiment. To compare the antioxidant property of C. dots with the raw jeera samples, 10 mg/ml of stock solution of raw jeera sample was prepared from lyophilised methanolic extract of jeera. Precisely, different dilutions of C. dots and raw jeera were incubated with 1 ml of 100 μM methanolic solution of DPPH. The final volume of all the solutions was maintained to be 2.5 ml. The samples along with appropriate standard solutions were incubated for 30 min in the dark environment. The decrease in absorbance due to the scavenging of DPPH radical was measured at 517 nm. The percentage radical scavenging activity of samples was calculated and the concentration at which 50% of the initial DPPH scavenged was noted from the graph.

$$\%\textbf{Scavenging activity} = (\mathbf{A_{blank}} - \mathbf{A_{solution}} / \mathbf{A_{solution}}) * \mathbf{100}$$

Where, A_{blank} and $A_{solution}$ are absorbance of the DPPH solution without and with the C. dots.

Synthesis of Cystamine Capped C. dots

Synthesis of Cysm-C. dots involved successful covalent bond formation between the free amino groups of cystamine and carboxyl groups of C. dots. The synthesis was carried out using the earlier reported methodology with slight modifications [30]. Firstly, 10 mg of carboxyl groups containing C. dots (1 mg/ml) were dissolved in 10 ml of PBS buffer of pH 7.4 (0.1 M). It was then kept for stirring by adding 4 ml aqueous solution of EDC (0.02 g, 0.1 mM) and NHS (0.01 g, 0.08 mM). EDC activates the carboxyl functional groups of C. dots. Stirring at room temperature was continued for next 24 h. To this solution, cystamine (10 mg, 0.12 mM) was added and the stirring was continued further for 24 h. The obtained solution was then dialysed (MWCO 1KD) for 24 h. against distilled water to remove excess reactants and the final product was collected after lyophilisation.

Cytotoxicity Study of C. dots

The evaluation of cytotoxicity of C. dots was done by MTT (3-(4,5-dimethythiazol2-yl)-2,5-diphenyl tetrazolium bromide) assay. MCF-7 cells (breast cancerous cells) were taken as the model cells for bioimaging. To understand the biocompatibility of C. dots towards these cells the cytotoxicity studies were carried out. MCF-7 cells were stained with 0.1% trypan blue and cell counting was done using neubauer chamber. These cells were seeded in a microtitre plate at a density of 5000 cells per well and cultured in a humidified incubator at 37 °C for 24 h under a 5% CO_2 atmosphere in DMEM (Dulbecco's modified Eagle's medium) supplemented with 10% FBS (fetal bovine serum) and 1% streptomycin. Fresh medium containing a range of concentration of C. dots (0–1 mg/ml) were added to each well and incubated for 24 h. 20 μl of MTT solution was added to each well and incubated at 37 °C for 5–6 h. The microplate reader (Thermo scientific MULTISKAN GO V3.2) was used to measure the absorbance at 570 nm. The absorbance of treated cells and control were compared to obtain percent cell viability.

Overnight grown culture of *Staphylococcus aureus* NCIM 5021(equivalent collection number ATCC 25923), *Staphylococcus aureus* S8 (a clinical isolate), *Pseudomonas aeruginosa* NCIM 5029(equivalent collection number ATCC 27853) and *Pseudomonas aeruginosa* PAW1 (a clinical isolate) in Luria Bertani broth at 37 °C was used to adjust the O.D. at 1×10^5 CFU/ml respectively. Minimum Inhibitory Concentration (MIC) of C. dots against above mentioned strains was determined at concentrations ranging from 1000 to 3000 μg/ml by broth microdilution method in microtitre plate using Muller Hinton Broth (MHB). The plates were incubated at 37 °C for 24 h. Absorbance was read at 540 nm using microtitre plate reader (Shimadzu UV1800 Spectrophotometer, Japan).

Bioimaging of MCF-7 Cells and Bacterial Cells

MCF-7 cells were seeded in a density of 0.3×10^6 cells/ 35 mm plate (with coverslips) in a culture DMEM medium supplemented with 10% fetal bovine serum and 1% streptomycin. They were then incubated for 24 h after which the culture media was removed and 1 mg/ml of C. dots was added. This was incubated further for 24 h and washed with the culture medium. The confocal microscope, NIKON A1 R, was used to obtain the fluorescence images.

Staphylococcus aureus S8(Gram positive) and, *Pseudomonas aeruginosa* PAW1(Gram negative) were employed for the bioimaging studies of the bacterial cells. O.D. adjusted culture was incubated with 1 mg/ml of C. dots

for 2 h. This was further used for the slide preparation and was observed under fluorescence microscope using excitation wavelength of 365–395 nm, 450–490 nm and 545–570 nm (ZEISS Axio Scope A1).

Results and Discussion

Jeera is the dried seed of the herb *Cuminum cyminum*, which is widely used as a spice condiment in South East Asia reaching up to India. The nutritional data shows the presence of proteins, carbohydrates, vitamins and fats. It is a traditional herb used for promoting digestion and reducing food-borne infections [27]. It is also used in the treatment of diarrhoea, dyspepsia and jaundice. The presence of plant compounds like terpenes, phenols, flavonoids and alkaloids makes cumin seeds a good source of antioxidants [28]. The obtained C. dots were then subjected to characterisation study and the properties were studied in detail.

Characterization of fluorescent C. dots

The one pot hydrothermal treatment of the carbon source, jeera without any passivating agents resulted in fluorescent C. dots. The size and the surface morphology features were obtained by TEM and SEM analysis respectively as shown in Fig. 1a, b. The TEM images clearly indicate that the C. dots obtained are with near spherical shape, well dispersed with average size distribution in the range of 6–9 nm. The magnified SEM images of the C. dots are shown in Fig. S1(B). The composition of the C. dots were obtained from EDX elemental analysis which showed the presence of C, O and N elements with the mass % of 70.61, 27.04 and 2.35 respectively (Fig. S1(A)). The elemental mapping shows the distribution of these elements in the C.dot frame work (Fig. 1c). The DLS size distribution is shown in Fig. S 5(B).

FTIR spectrum was taken to examine the functional groups on C- dots and shown in Fig. 2. The characteristic absorption peak shown at 3202 cm^{-1} indicate O–H/N–H stretching bands,

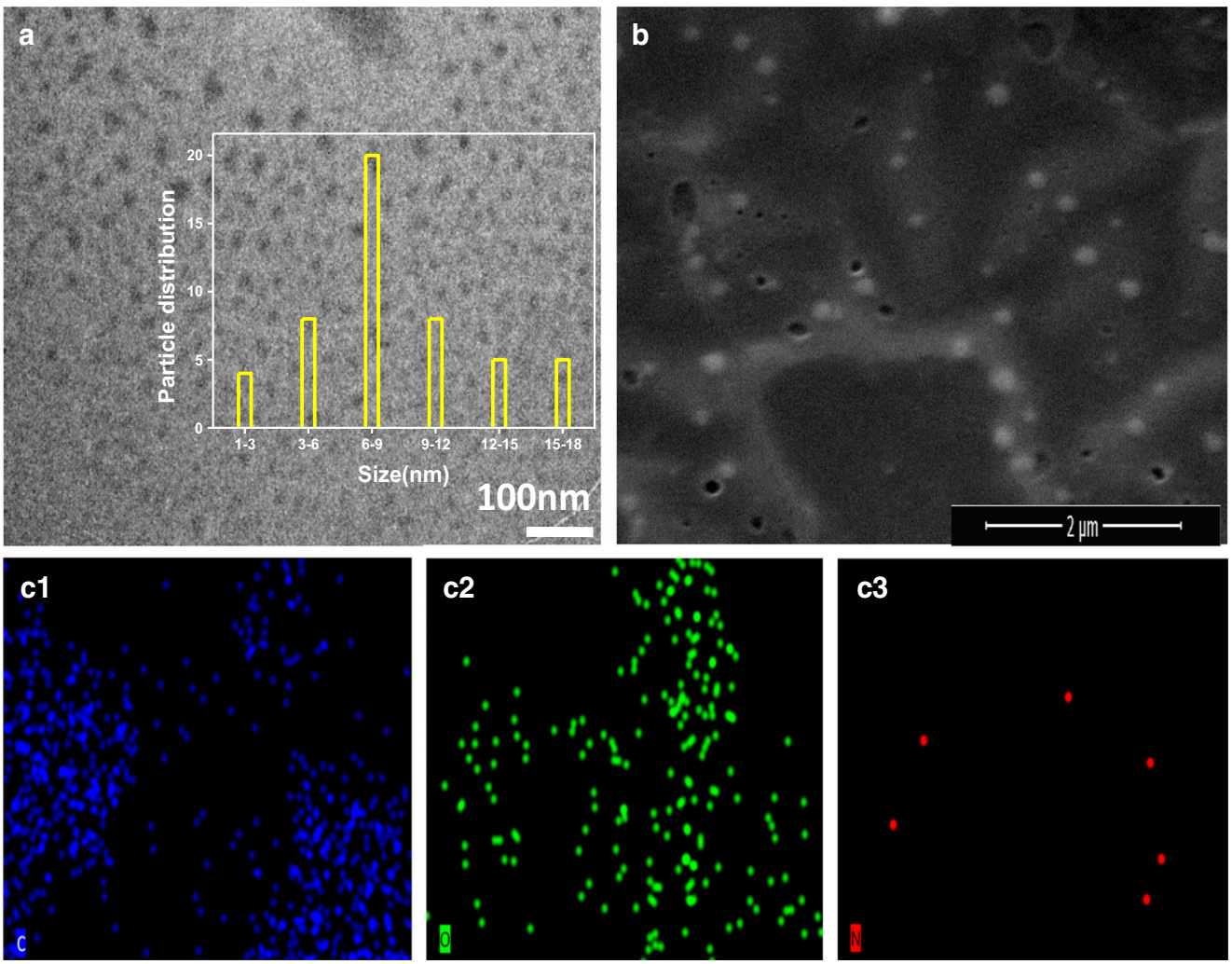

Fig. 1 a, b TEM and SEM(white dots represents C. dots) image of C-dots. The inset displays the histogram of the size distribution of C. dots (C) Elemental mapping of C. dots. (1–3) Individual elemental distribution (blue for carbon, green for oxygen and red for nitrogen)

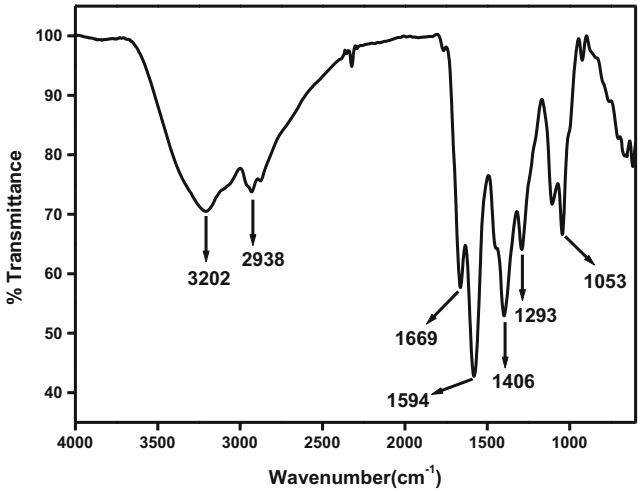

Fig. 2 FTIR spectrum of C. dots

whereas peak at 2938 cm^{-1} corresponded to C–H stretching vibration. The peak at 1669 cm^{-1} matched to C=O stretching vibrations of carboxyl groups present on the C. dot surface. The characteristic absorption at 1293 cm^{-1} was assigned to C–OH stretching. The peak at 1594 cm^{-1} shows the N–H vibration. Furthermore, the peaks at 1456 cm^{-1} and 1050 cm^{-1} attributed to bending vibrations of C–H and C–O bonds in carboxyl groups respectively. These spectral details clearly indicate the presence of carboxyl and hydroxyl groups on C. dots surface.

The analysis of UV-vis spectra (Fig. 3a) exhibited a distinct peak at 273 nm and a tiny bulge at 320 nm, indicating the π-π* transition of C=C and n-π* transition of C=O groups in C-dots respectively [18]. The aqueous soluble C-dots showed a remarkable blue fluorescence under UV light and a maximum emission intensity at 434 nm was observed when excited at 360 nm (Fig. 3b). A detailed inspection of C-dots fluorescence spectra from 260 nm to 360 nm showed excitation dependant emission spectra with a red shift in the emission maximum. An enhancement in fluorescence intensity was observed till an excitation wavelength of 360 nm, further excitation wavelengths resulted in a gradual decrease in intensity. This interesting phenomena can be mainly attributed to the surface defects or emissive traps of C-dots [29]. An excitation spectra of C. dots at different emission wavelength were also shown (Fig. S2(A)). The quantum yield (Q.Y) of the C-dots obtained from jeera was found to be 5.33% when measured against quinine sulphate as a standard reference (Fig. S3(A)). The C-dots obtained from jeera showed a negative zeta potential value of −10.34 (Fig.S3(B)). This high negative value showed the good colloidal stability of the C-dots which can be utilised for biological application. Furthermore, it clearly indicates the presence of hydroxyl and carboxyl groups on C. dots surface as confirmed by the IR analysis.

XRD pattern portrayed a broad peak at $2\theta = 22.5°$ representing the (002) planes of graphitic carbon with amorphous characteristics (Fig. 4a). Apart from this, the pH and photostability studies of C-dots were carried out. pH is a key factor that must be considered when C. dots are being applied in biomedical field. Hence we have studied the effect of pH on C. dots by observing the fluorescence spectra at various pH. The fluorescence intensity was found to be slightly decreased in highly acidic and basic pH and maximum intensity was observed at neutral pH (Fig. 4b) The C. dots were able to retain 90% photo stability after 3 h. of continuous irradiation by Xe lamp (Fig. S4(A)). The life time of the C. dots obtained from jeera was found to be 9.5 ns (Fig.S4(B).

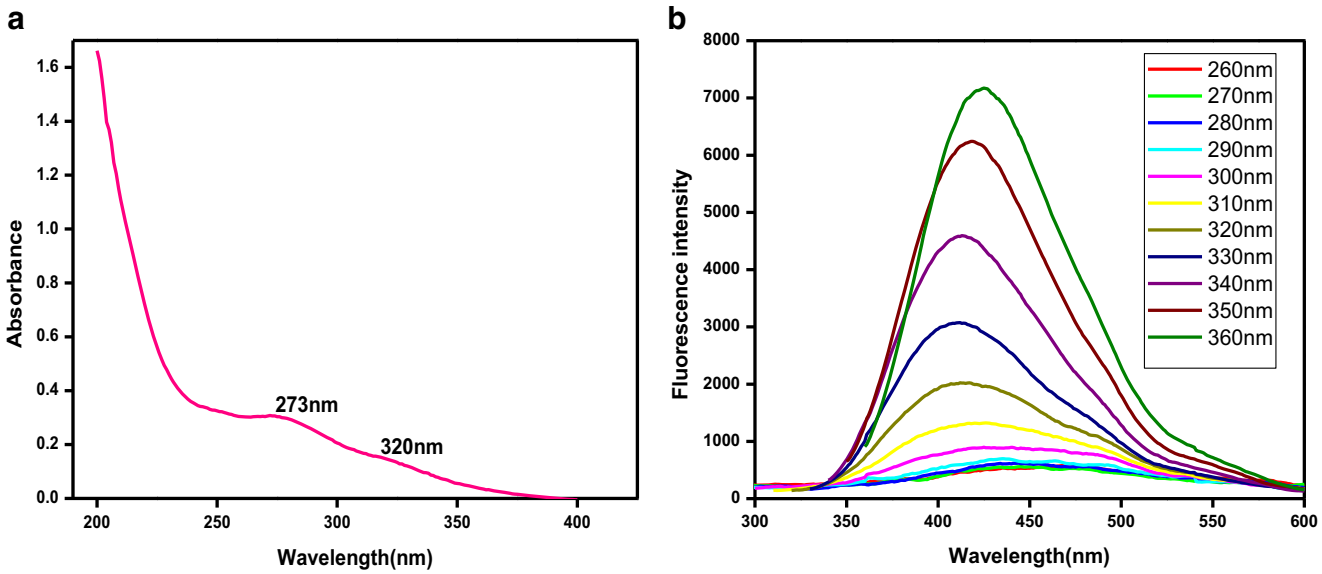

Fig. 3 (**a**) Absorbance spectrum, (**b**) Emission spectra of C. dots under different excitation wavelengths from 260 to 360 nm

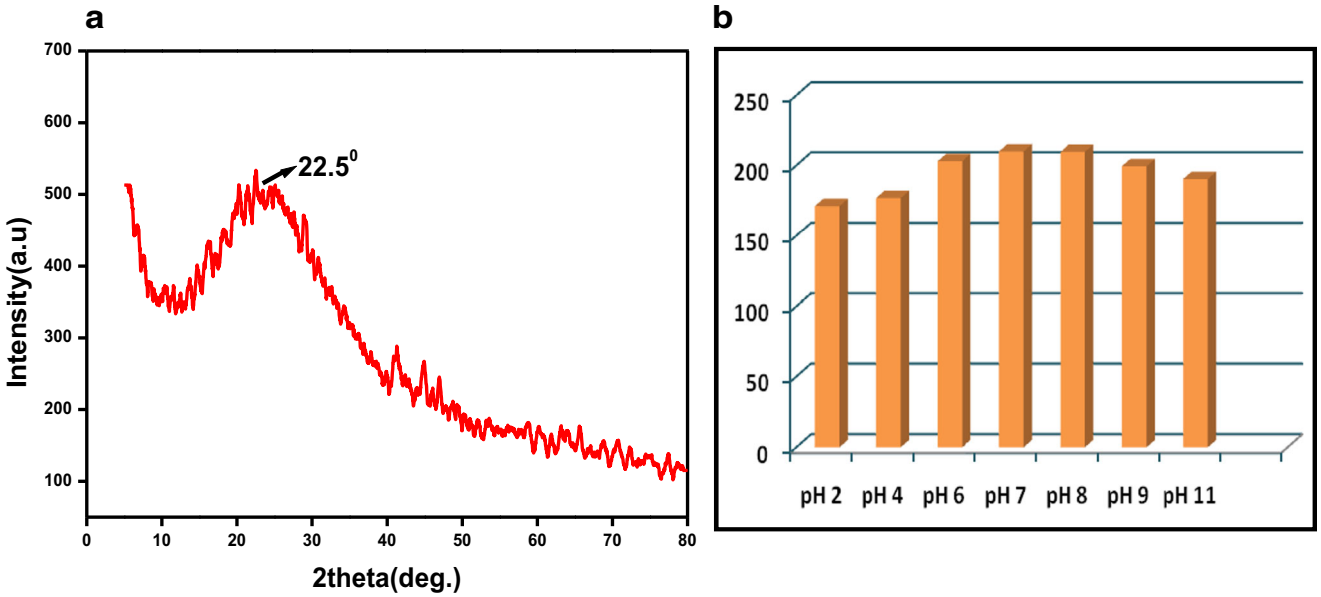

Fig. 4 **a** XRD spectrum of C. dots and **b** Effect of pH on the fluorescence emission of C. dots

Antioxidant Activity of C. dots - DPPH Assay

Free radicals and other reactive oxygen species are generated in our body as a by-product of various detoxification reactions. Antioxidants are compounds which can effectively neutralise or scavenge free radicals [28]. DPPH assay is one of the most common method employed to assess the antioxidant activity of a compound. DPPH is a deep purple coloured compound, consists of stable free radicals which can absorb an electron or hydrogen to become a stable diamagnetic molecule. Antioxidant property of methanolic extract of jeera is already reported [22]. Based on the assumption that major compounds present in the precursor will partially remain inside or at the surface of the C-dots, after the hydrothermal treatment, the antioxidant properties of C. dots were investigated. Here, we have compared the antioxidant property of raw jeera sample and the C-dots obtained from jeera. Same reaction conditions were followed in both the cases where different concentration of jeera and C.dot solutions were added to 100 μM DPPH solution (Fig. 5). A decrease in absorbance at 517 nm was noted with increase in concentration of C. dots and raw jeera from 220 to 1540 μg/ml. Increase in antioxidant activity was observed in both cases. C. dots showed an increase in antioxidant activity upto 80% where as raw jeera samples showed 65% at the same concentration. From the graph the EC_{50} values were estimated and was found to be 1.2 mg/ml for C. dots and 14 mg/ml for raw jeera. The significant number of hydroxyl groups produced during carbonisation process can be considered as a reason for the enhanced antioxidant activity of C. dots.

Modification of C-dots for Selective Cr (VI) Sensing

The C. dots synthesised from natural sources has inspired the research community due to their attributes like easy availability and cheap precursors, facile synthetic methodology and properties like exceptional aqueous solubility, remarkable photostability, low toxicity etc. To study the optical sensing ability of C. dots towards metal ions, 10 metal ions were selected (each having 0.1 mM concentration). The C. dots was not found to be selective, since the metal ions like Fe (III), Cr (VI), Hg (II) and Cu (II) were able to influence the fluorescence of C. dots as per the results obtained (Fig. 10a). Some of the recent studies also point out to the poor selectivity

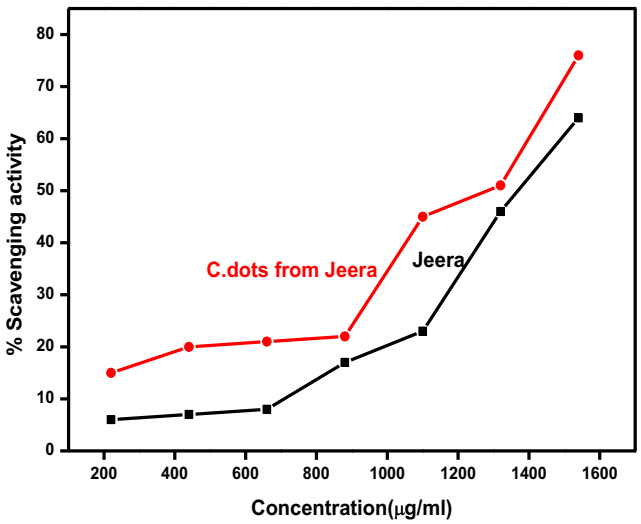

Fig. 5 Comparison of the antioxidant activity showed by C. dots from jeera and raw jeera as examined by DPPH free radical scavenging assay

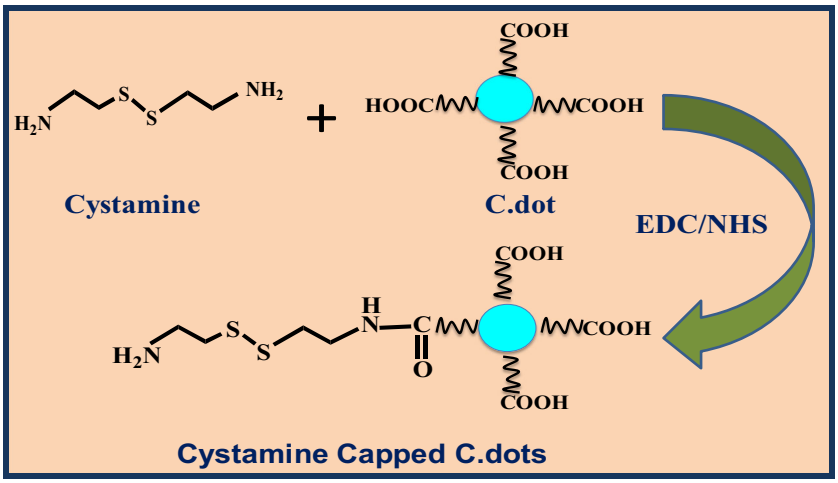

Fig. 6 Scheme of Capping of C. dots with cystamine in presence of capping agent EDC/NHS to form Cysm-C. dots

of C. dots towards metal ion sensing [30]. So it remained as a great challenge to modify these C. dots for the selective sensing of metal ions.

EDC/NHS Coupling Chemistry Using Cystamine

Mainly two modification strategies have been put forward by researchers for enhancing the usability of C. dots. First, tuning the fluorescence properties of C. dots for effectively implementing it in bioimaging, photocatalyst, opto electronic devices etc. The second one, which is more striking, is to conjugate the C. dots with functional groups which will result in a newly designed functional material for creative application in specific task [31].

Here, we have attempted to crosslink C. dots with cystamine by carbodiimide chemistry where EDC is used as an effective cross linking agent along with NHS. The carboxyl groups of C-dots were covalently conjugated with free amino groups of cystamine through a successful covalent cross linking reaction. EDC act as an efficient cross linking agent by forming an ester with the carboxyl groups of C. dots which are easily hydrolysable. To prevent the hydrolysis, these esters were stabilised by the addition of NHS. When treated with amino groups of cystamine, it formed a stable amide linkage. The non conjugated C. dots and other by-products could be easily removed by dialysis. A schematic illustration of coupling of C. dots with Cystamine using EDC/NHS is shown in Fig. 6.

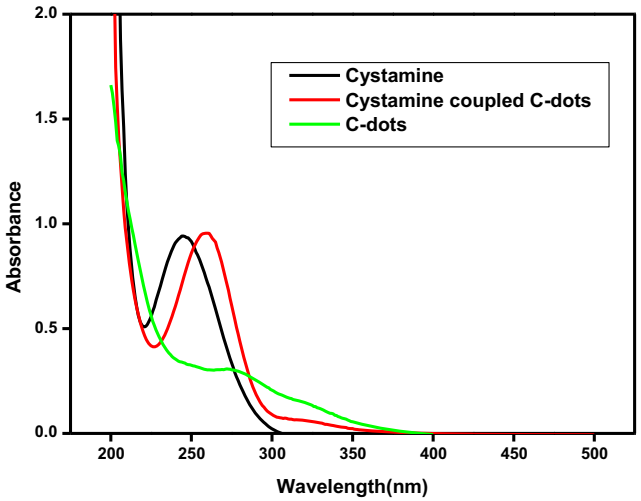

Fig. 7 UV–vis absorption spectra of C. dots, Cystamine and Cystamine coupled C. dots (Cysm-C. dots) showing λ_{ex} at 273 nm, 245 nm and 260 nm respectively

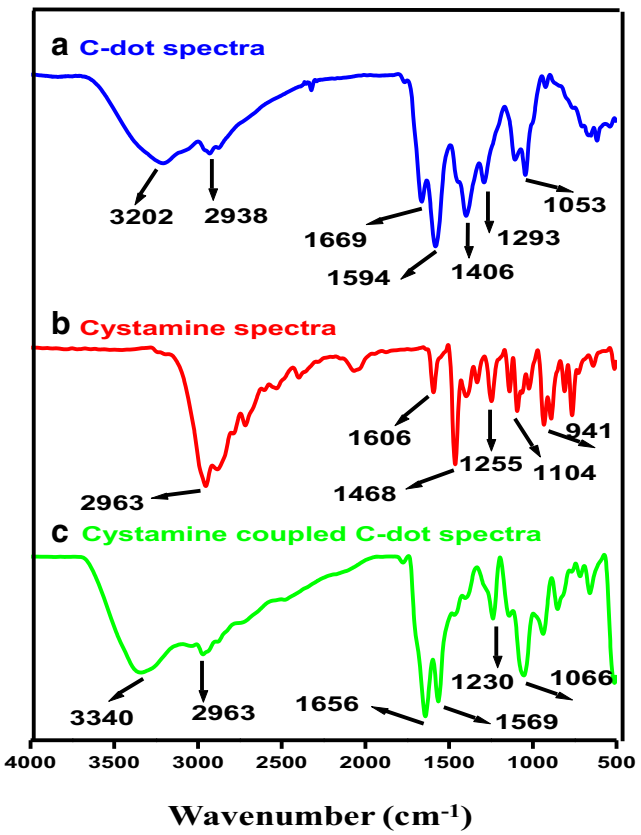

Fig. 8 FTIR spectra of A) C. dots, B) Cystamine and C) Cysm-C. dots

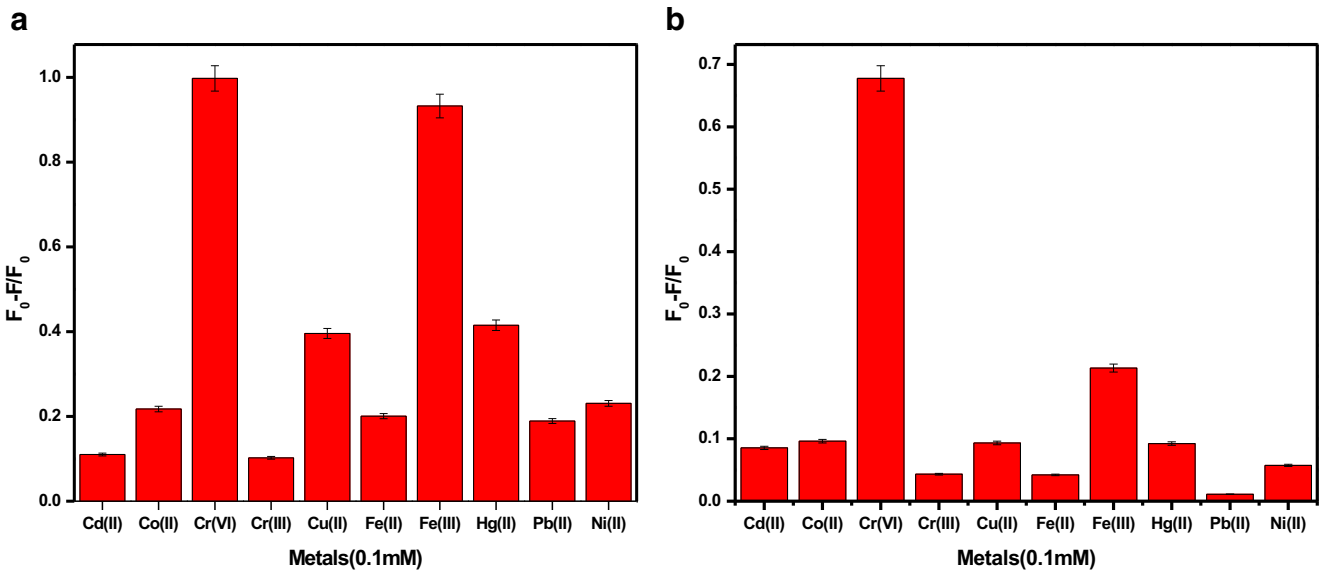

Fig. 9 **a** The quenching ability of different metal ions on the fluorescence of C. dots **b** the selective quenching of the emission intensity of Cysm-C.dot system by Cr(VI)

The functionalisation of cystamine on the surface of C. dots were confirmed by UV-visible, FTIR, zeta potential values. The UV-visible spectrum of Cysm-C. dots showed a characteristic absorption peak at 260 nm which was slightly red shifted from the original cystamine peak at 245 nm. This could be due to the conjugative interaction of C. dots with cystamine (Fig. 7). The successful functionalisation of cystamine on the surface of C. dots was supported by the FTIR spectra (Fig. 8). Cysm-C. dots showed a characteristic peak at 1656 cm^{-1} which clearly indicate the C=O stretching from amides (–$CONH_2$) formed during the crosslinking. A distinct peak of C–OH stretching at 1293 cm^{-1} in the C.dot structure has disappeared from the Cysm-C-dots spectra due to the binding of carboxyl groups with amines. The zeta potential value of Cysm-C. dots were found to be −1.03 which was much higher than the zeta potential of C. dots suggesting the loss of negatively charged carboxyl groups in coupled interaction (Fig.S4A).

Selective Sensing of Cr(VI) by Cysm-C. dots System

Figure 9b shows the fluorescence emission response of the Cysm-C.dot system towards various metal ions. Ten environmentally important metal ions were selected for the analysis. When compared to unconjugated C. dots as shown in Fig. 9a, cysm-C.dot system showed much selective quenching

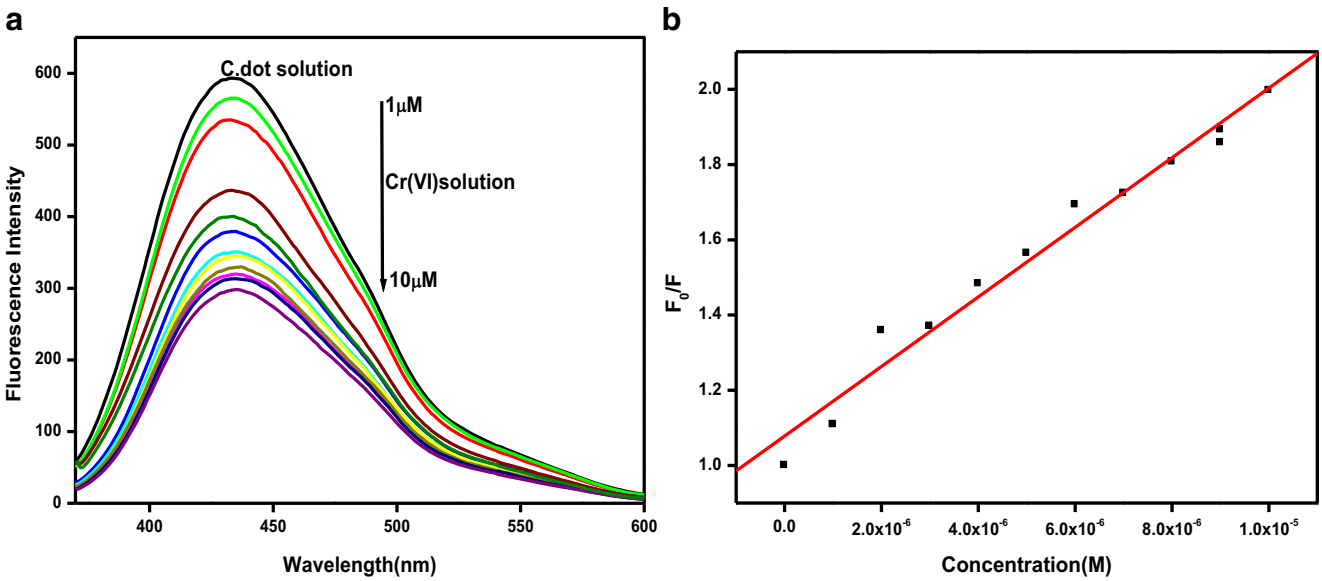

Fig. 10 **a** The PL spectra of Cysm-C. dots in presence of varying concentration of Cr(VI) from 1 to 10 μM and **b** Stern-Volmer plot

Table 1 Detection of spiked Cr (VI) and total Cr in tap water

Tap water samples	Cr (III) added(μM)	Cr (VI) added (μM)	Cr (VI) found (μM)	Total Cr found (μM)	Cr (III) calculated	Recovery% Cr (III) – Cr (VI)	
1	3	3	3.1	5.92	2.82	94	103
2	4.5	4.5	4.62	9.05	4.43	98	102

response with Cr(VI). The quenching can be mainly due to the charge transfer interaction between Cysm-C.dot and Cr(VI). The photo physical properties of C. dots depend on the surface state. It was reported that the interaction of metal cations with the capping layer of C. dots can enhance or quench the fluorescence of C. dots through the ionic interaction of capping layer with metals [32, 33]. The sensing of Cr(VI) using cystamine take place through the formation of Cr(VI)-Cystamine complex which in turn results in the aggregation of uncapped C. dots. The quenching of fluorescence of C. dots can be mainly due to this reason. This presumption of uncapping of Cysm-C. dots system in presence of Cr(VI) can be verified by the IR spectrum where the peaks of Cysm-C. dots were considerably reduced in intensity (Fig.S4B). Therefore, the fluorescence quenching can be ascribed to the complex reaction of Cr(VI) and the surface cystamine capping layer of the C. dots.

To demonstrate the viability of using Cysm-C. dots as a sensing probe for the detection of Cr (VI) in water, the emission spectra of Cysm-C. dots ($\lambda_{em} = 440$ nm) in the presence of varying concentrations of Cr (VI) ions were recorded. Upon adding Cr(VI) ions, a gradual decline of emission intensity was clearly seen, suggesting that the fluorescence of cysm-C.dot system was sensitive to Cr (VI) ions (Fig. 10a).

The quenching efficiency of Cr (VI) towards Cysm-C. dots system was obtained from Stern-Volmer quenching plot (Fig. 10b) using the equation,

$$F_0/F = 1 + K_{sv}[C] \quad (1)$$

Here, F_0 and F are fluorescence intensities in the absence and presence of metal ion. K_{sv} is the Stern-Volmer quenching constant and [C] is the concentration of metal ions. Using the 3σ rule the detection limit was found to be 1.57 μM (80 ppb). The Cysm-Cdot system showed an improved LOD when compared to our previous system with LOD 1.9 μM (100 ppb).

Total Cr Determination and Real Sample Analysis

A simple and precise analytical procedure is required for the Cr speciation and total Cr content in environmental samples as their toxicities are wide apart. Here, an alkaline oxidation procedure was followed using H_2O_2/NaOH where Cr (III) was successfully converted into Cr (VI).

The feasibility of C. dots for detecting Cr (VI) and total Cr in real water samples, a systematic study was conducted with tap water sample spiked with standard solutions containing different concentrations of Cr (VI) and Cr (III). Calibration plot was developed with F_0/F along y axis and metal ion concentration along x axis. The solution which was spiked with two different concentration of Cr (III) and Cr (VI) (3 and 4.5 μM) and was predicted using the calibration graph (Table 1).

Cell Viability and Cell Imaging Applications of C. dots for MCF-7Cells

Considering the excellent optical properties and physiological characteristics like good water dispersibility, lasting photo stability etc. of the C. dots synthesised from jeera, their potential for in vitro multicolour fluorescence imaging of breast cancer cells (MCF-7) were evaluated. The cytotoxicity play a key role in the applicability of any system for bioimaging of cells. The cytotoxicity of C. dots was evaluated by the MTT assay for MCF-7 cells. Figure 11 indicated that the cell viability using C-dots towards MCF-7 cells was 80%, even after 24 h incubation with C. dots at a concentration of 1 mg/ml. Initially the survival rate was reduced to 90% when compared with control but was able to sustain almost the same cell viability at higher concentration also. Essentially, the above results portray the biocompatibility of C. dots for bioimaging.

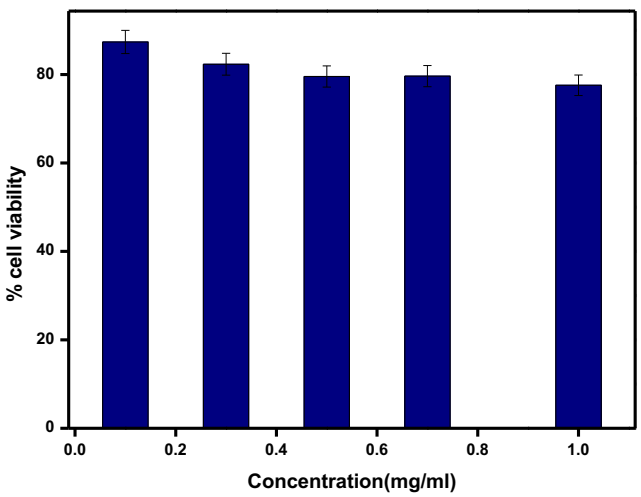

Fig. 11 Cell viability evaluation of MCF-7 cells after 24 h of incubation with increasing concentrations of C. dots

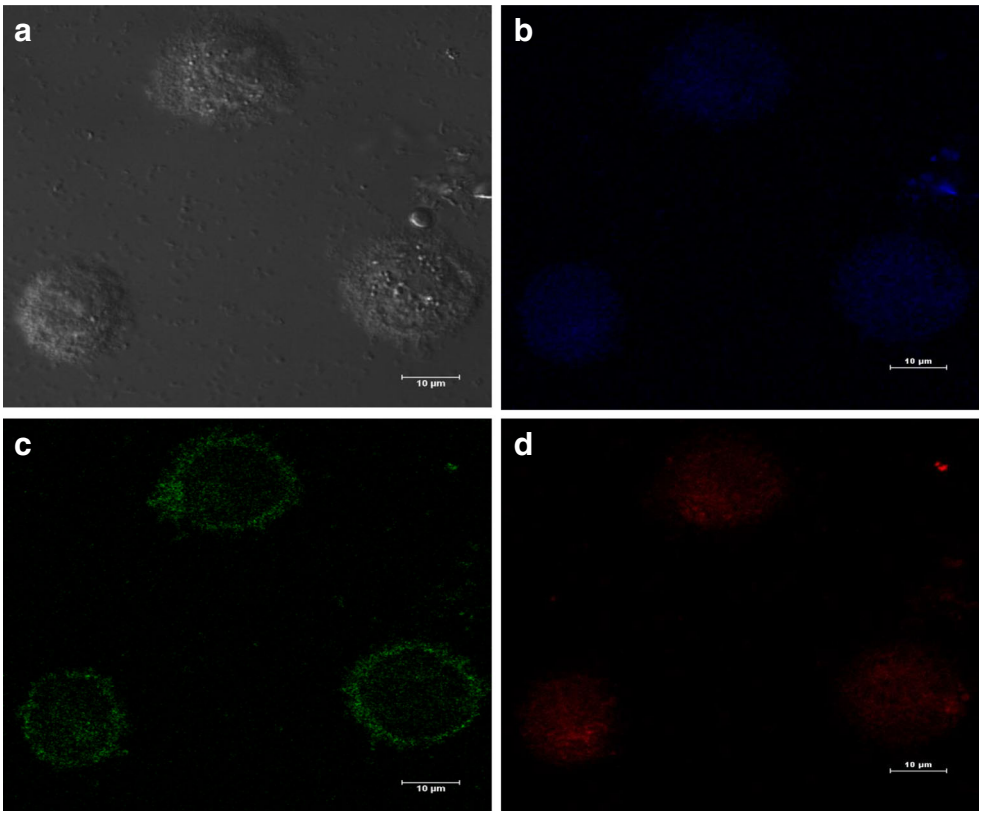

Fig. 12 Fluorescence imaging of MCF-7 cells using C. dots after 24 h of incubation with **a** Bright field image **b** with excitation lasers at 405 nm **c** 488 nm and **d** 561 nm and collecting the emitted fluorescence in the blue, green and red areas

Based on the above results of cell viability study, the fluorescence imaging study of MCF-7 cells were carried out after incubation with C. dots for 24 h at a concentration of 1 mg/ml. As shown in the Fig. 12, even though there is a bulk allocation of C. dots in the cell membrane, a part of the C. dots was found to be diffused

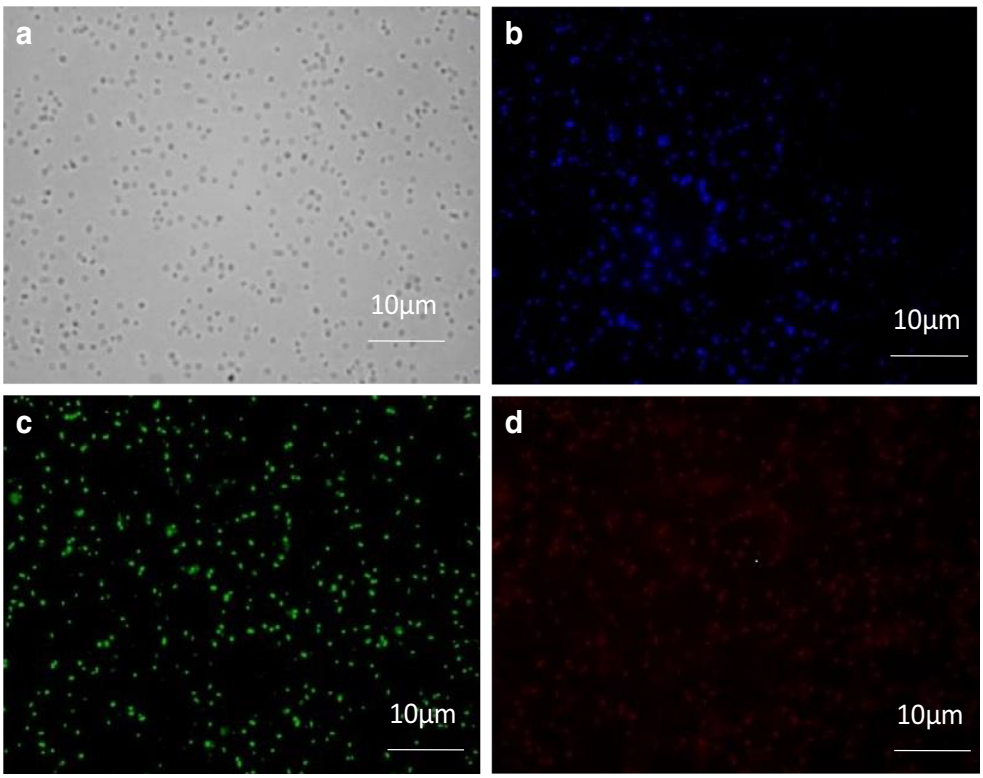

Fig. 13 Fluorescent microscopic images of *Staphylococcus aureus* after 1 h of incubation with C. dots **a** Bright field image. Fluorescence image taken using excitation filters **b** 365–395 nm(blue) **c** 450–490 nm(green) and **d** 545–570 nm(red)

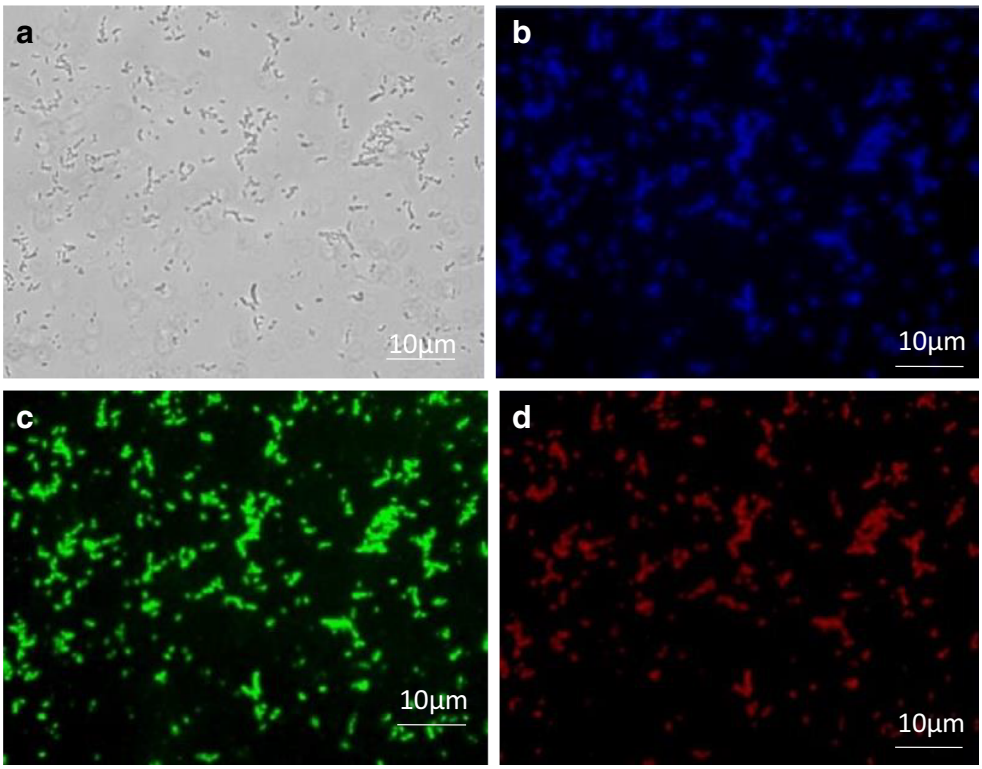

Fig. 14 a-d) Fluorescent microscopic images of *Pseudomonas aeruginosa* after 1 h of incubation with C. dots. **a** Bright field image. Fluorescence image taken using excitation filters **b** 365–395 nm(blue) **c** 450–490 nm(green) and **d** 545–570 nm(red)

into the cytoplasm and the nuclear area of the cells. Thus, a more efficient uptake of C. dots obtained from jeera by MCF-7 cells was observed compared to our previous work where there was a limited diffusion of C. dots into the nuclear area of the cells.

Imaging of Bacterial Cells Using C. dots

The MIC value was found to be 2.5 mg/ml for the above mentioned strains. These results revealed that the prepared C-dots did not behave as bacteriostatic and bactericidal agents. After incubation of *Staphylococcus aureus* S8 and *Pseudomonas aeruginosa* PAW1 along with C. dots respectively, the fluorescence microscopy revealed that blue fluorescence was observed when excited at 365-395 nm wavelength, green fluorescence was observed when excited at 450-490 nm wavelength and red fluorescence at 545-570 nm wavelength (Figs. 13 and 14). This indicates that the prepared C-dots were effectively taken up by the bacterial cells, and also shows their potential to be employed as fluorescent imaging agents for bacterial cells.

Conclusion

To conclude, we have developed a green and economically feasible Cr(VI) sensor by synthesising C. dots from jeera by hydrothermal carbonisation. The synthesised C. dots were highly fluorescent, photo stable and soluble in water. C. dots were characterised by different techniques like TEM, SEM, XRD, FTIR etc. The antioxidant properties of C. dots obtained from jeera was determined by DPPH assay and was compared with the antioxidant properties of raw jeera. To employ the C. dots as a selective sensor for Cr (VI), it was capped with cystamine by EDC/NHS coupling agents. The system was found to be selective and sensitive for Cr(VI) detection with a minimum detection value of 1.57 μM. Inspired by the remarkable properties of C. dots like good water solubility, photo stability, and bio compatibility, the C. dots were effectively used for the imaging of MCF-7 cells and bacterial cells.

Acknowledgement Physics department, Savitribai Phule Pune University, Pune is acknowledged for TEM facility.

References

1. Shen JH, Zhu YH, Yang XL, Li CZ (2012) Graphene quantum dots: emergent nanolights for bioimaging, sensors, catalysis and photovoltaic devices. Chem Commun 48:3686–3699
2. Coto-Garcia AM, Sotelo-González E, Fernández-Argüelles MT, Pereiro R, Costa-Fernández JM, Sanz-Medel A (2011) Nanoparticles as fluorescent labels for optical imaging and sensing in genomics and proteomics. Anal Bioanal Chem 399:29–42
3. Huang H, Li C, Zhu S, Wang H, Chen C, Wang Z, Bai T, Shi Z, Feng S (2014) Histidine-derived nontoxic nitrogen-doped carbon

dots for sensing and bioimaging applications. Langmuir. 30:13542–13548
4. Baker SN, Baker GA (2010) Luminescent carbon nanodots: emergent nanolights, Angew. Chem. Int Ed 49:6726–6744
5. Sun YP, Zhou B, Lin Y, Wang W, Fernando KAS, Pathak P, Meziani MJ, Harruff BA, Wang X, Wang H, Luo PG, Yang H, Kose ME, Chen B, Veca LM, b Xie S.Y. (2006) Quantum-sized carbon dots for bright and colorful photoluminescence. J Am Chem Soc 128:7756–7757
6. De B, Karak N (2013) A green and facile approach for the synthesis of water soluble fluorescent carbon dots from banana juice. RSC Adv 3:8286–8290
7. Wang N, Wang Y, Guo T, Yang T, Chen M, Wang J (2016) Green preparation of carbon dots with papaya as carbon source for effective fluorescent sensing of Iron (III) and Escherichia coli. Biosens Bioelectron 85:68–75
8. Wang L, Zhou HS (2014) Green synthesis of luminescent nitrogen-doped carbon dots from Milk and its imaging application anal. Chem. 86:8902–8905
9. Shen J, Shang S, Chen X, Wang CDY (2017) Facile synthesis of fluorescence carbon dots from sweet potato for Fe^{3+} sensing and cell imaging. Mater Sci Eng C Mater Biol Appl 76:856–864
10. Sahu S, Behera B, Maiti TK, Mohapatra S (2012) Simple one-step synthesis of highly luminescent carbon dots from orange juice: application as excellent bio-imaging agents. Chem Commun 4: 8835–8837
11. Yang X, Zhuo Y, Zhu S, Luo Y, Feng Y, Dou Y (2014) Novel and green synthesis of high-fluorescent carbon dots originated from honey for sensing and imaging. Biosens Bioelectron 60:292–298
12. Sachdev A, Gopinath P (2015) Green synthesis of multifunctional carbon dots from coriander leaves and their potential application as antioxidants, sensors and bioimaging agents. Analyst. 140:4260–4269
13. Roshni V, Divya O (2015) Synthesis of carbon nanoparticles using one step green approach and their application as mercuric ion sensor. J Lumin 161:117–122
14. Roshni V, Misra S, Santra S, Divya O (2018) One pot green synthesis of C-dots from groundnuts and its application as Cr(VI) sensor and in vitro bioimaging agent. J Photochem 375:28–36
15. Zhang L, Xu C, Li B (2009) Simple and sensitive detection method for chromium(VI) in water using glutathione-capped CdTe quantum dots as fluorescent probes. Microchim Acta 16:61–68
16. Song Y, Zhu S, Yang B (2014) Bioimaging based on fluorescent carbon dots. RSC Adv 4:27184–27200
17. Mukesh KK, Mukeshchand T, Raju BG, Rohit S (2017) Graphene quantum dots from Mangifera indica: application in NearInfrared bioimaging and intracellular Nanothermometry, ACS sustainable Chem. Eng. 5:1382–1391
18. Vasimalai N, Boas VV, Gallo J, Cerqueira MF, Miranda MM, Costa-Fernández JM, Diéguez L, Espiña B, Fernández-Argüelles MT (2018) Green synthesis of fluorescent carbon dots from spices for in vitro imaging and tumour cell growth inhibition. Beilstein J Nanotechnol 9:530–544
19. Park SY, Lee HU, Park ES, Lee SC, Lee JW, Jeong SW, Kim CH, Lee YC, Huh YS, Lee J (2014) Photoluminescent green carbon Nanodots from food-waste derived sources: large-scale synthesis, properties, and biomedical applications, ACS Appl. Mater Interfaces 6:3365–3370
20. Kasibabu BSB, D'souza SL, Jha S, Singhal RK, Basu H, Kailasa SK (2015) One-step synthesis of fluorescent carbon dots for imaging bacterial and fungal cells. Anal Methods 7:2373–2378
21. Mehta VN, Jha S, Basu H, Singhal RK, Kailasa SK (2015) One-step hydrothermal approach to fabricate carbon dots from apple juice for imaging of mycobacterium and fungal cells. Sensors Actuators B Chem 213:434–443
22. Anita D, Gupta SK, Mittal A, Mahajan R (2012) A study of antioxidant properties and antioxidant compounds of cumin (Cuminum cyminum). Int J Pharm Biol Sci 3(5):1110–1116
23. Sultana S, Ripa FA, Hamid K (2010) Comparative antioxidant activity study of some commonly used spices in Bangladesh. Pak J Biol Sci 13(7):340–343
24. Ani V, Kamatham AN (2011) Antioxidant potential of bitter cumin (Centratherum anthelminticum (L.) Kuntze) seeds in in vitro models. BMC Complement Altern Med 11:1–8
25. Mohamed DA, Hamed IM, Fouda KA (2018) Antioxidant and antidiabetic effects of cumin seeds crude ethanol extract J. Biol Sci 18(5):251–259
26. Nadeem M, Riaz A (2012) Cumin (Cuminum cyminum) as a potential source of antioxidants. PAK J FOOD SCI 22(2):101–107
27. Khanduja KL, Bhardwa A (2003) Stable free radical scavenging and antiperoxidative properties of resveratrol compared in vitro with some other biflavanoids. Indian J Biochem Biophys 40:416–422
28. Shahidi F (2000) Antioxidants in food and food antioxidants. Nahrung. 3:158–163
29. Xu Q, Zhao J, Liu Y, Pu P, Wang X, Chen Y, Jao C, Chen J, Zhou H (2015) Enhancing the luminescence of carbon dots by doping nitrogen element and its application in the detection of Fe(III) J. Mater Sci 50:2571–2576
30. Li Y, Zhang ZY, Yang HF, Shao G, Gan F (2018) Highly selective fluorescent carbon dot probe for mercury(II) based on thymine-mercury(II) –thymine structure. RSC Adv 8:3982–3988
31. Zhao X, Zhang J, Shi L, Xian M, Dong C, Shuang S (2017) Folic acid-conjugated carbon dots as green fluorescent probes based on cellular targeting imaging for recognizing cancer cells. RSC Adv 7: 42159–42167
32. Luo PG, Sahu S, Yang ST, Sonkar SK, Wang J, Wang H, LeCroy GE, Cao L, Sun YP (2013) Carbon "quantum" dots for optical bioimaging. J Mater Chem B 1:2116–2127
33. Xia YS, Zhu CQ (2009) Interaction of CdTe nanocrystals with thiol-containing amino acids at different pH: a fluorimetric study. Microchim Acta 164:29–34